

AN OVERVIEW OF POWER DISSIPATION AND CONTROL TECHNIQUES IN CMOS TECHNOLOGY

N. B. ROMLI, K. N. MINHAD*, M. B. I. REAZ, MD. S. AMIN

Department of Electrical, Electronic and Systems Engineering, Faculty of Engineering and Built Environment, Universiti Kebangsaan Malaysia, 43600 Bangi, Selangor, Malaysia

*Corresponding Author: khairunnisa.minhad@gmail.com

Abstract

Total power dissipation in CMOS circuits has become a huge challenging in current semiconductor industry due to the leakage current and the leakage power. The exponential growth of both static and dynamic power dissipations in any CMOS process technology option has increased the cost and efficiency of the system. Technology options are used for the execution specifications and usually it depends on the optimisation and the performance constraints over the chip. This article reviews the relevant researches of the source or power dissipation, the mechanism to reduce the dynamic power dissipation as well as static power dissipation and an overview of various circuit techniques to control them. Important device parameters including voltage threshold and switching capacitance impact to the circuit performance in lowering both dynamic and static power dissipation are presented. The demand for the reduction of power dissipation in CMOS technology shall remain a challenging and active area of research for years to come. Thus, this review shall work as a guideline for the researchers who wish to work on power dissipation and control techniques.

Keywords: CMOS, Dynamic power, Logic speed, Low power, Static power.

1. Introduction

The evolution of CMOS integrated circuit is a major milestone in the history of modern technology for both high performance and portable applications. Power dissipation is an important parameter in the design of CMOS ICs [1]. It requires high consideration in emerging technologies such as ultra-wideband (UWB) and radio frequency identification (RFID) [2-6] as well as wireless sensor networks (WSN) and short or long-range communication devices [7-9].

In CMOS technology, power dissipation mainly contributed by static and dynamic

Nomenclatures

C	Switched capacitance
C_G^i	Gate capacitance of i_{th} fan-out
C_{out}	Output capacitance
C_{wire}	Capacitance of the driven connections
g	Gate logical effort $g = C_{ig}/C_{sv}$
I_G	Gate oxide tunnelling leakage
I_{GIDL}	Gate induced drain leakage
I_H	Gate current due to hot-carrier injection
I_0	Depends on device dimensions
I_{REV}	Reverse-bias source/drain junction leakage
I_{SUB}	Sub threshold leakage
f_{clk}	Clock frequency
P	Power consumed
P_{switch}	Power supply on per charge or discharge
p	Parasitic power dissipation $p = C_p/C_{sv}$
t_{ox}	Oxide thickness
V	Supply voltage
VDD	Circuit input power supply voltage
V_{ds}	Drain-to-source voltage
V_{gs}	Gate-to-source voltage
V_{OX}	Potential across the oxide
V_T	Thermal voltage
V_{th}	Threshold voltage

Greek Symbols

α	Activity factor
α_{nm}	Normalised activity factor $\alpha_{nm} = \alpha_g \alpha_v$

power. The main components that affect power dissipation are capacitive load currents, short circuit currents and leakage currents [10]. Static power dissipation occurs due to leakage currents and subthreshold currents that contribute a small percentage to the total power consumption. Five main sources of leakage currents in CMOS transistors are subthreshold leakage (I_{SUB}), gate oxide tunnelling leakage (I_G), reverse-bias source/drain junction leakages (I_{REV}), gate induced drain leakage (I_{GIDL}) and gate current due to hot-carrier injection (I_H) [11, 12]. The following section will further discuss the details.

2. Background

Leakage current has become major factor that affect the power consumption as the technology advances into the sub-100 nm regime. Figure 1 depicts major contributors to the leakage current in NMOS transistor. The sub-threshold leakage (I_{SUB}) is one of the important parameters to consider. It is the current between drain and source in transistor that occurs due to weak inversion conduction when gate voltage becomes below V_{th} [13] due to the diffusion current of minority carrier in the transistor if the transistor is not completely turned off [14].

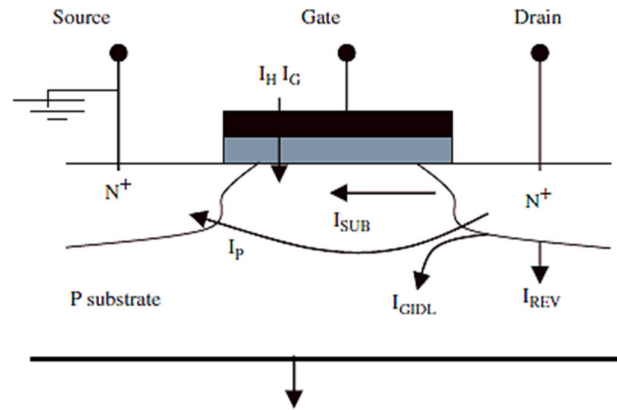


Fig. 1. Leakage current in NMOS transistor.

Gate oxide tunnelling current (I_G) is another parameter. As the oxide thickness scaling down, field oxide across the gate penetrates the electron from gate to substrate and vice versa. However, the increase of high electric field cause the electrons and holes gain sufficient energy to overcome the interface potential, hence it makes direct tunnelling current through transistor gate insulator. This gate leakage current depends on the potential across of the oxide, V_{ox} and oxide thickness, t_{ox} .

On the other hand, a small amount of currents flow in p-n junction between source/drain and substrate in reverse bias cause the junctions to leak which known as I_{REV} [15]. This is due to the high doping concentration that causes the tunnelling of electrons across the p-n junctions. The doping concentration and junction areas frequently trigger reverse-bias source/drain junction's leakage problem. Moreover, high electric field effect in the drain junction of the CMOS transistor causes the leakage current. The gate induced drain leakage current I_{GIDL} increases when thinner oxide and higher supply voltage are used. Thus, one of the techniques to control I_{GIDL} is via controlling the doping concentration in the drain of the transistor. The carriers which trapped in the oxide layer change the threshold voltage and subthreshold current. Here, the injection of electrons are more common than holes as electrons have both effective mass and lower barrier height of holes [16]. Thus, to control the leakage is by decreasing the proportion supply voltage to the device dimension.

3. Source of Dissipation in CMOS and Control Techniques

Dynamic power dissipation is the power consumed by CMOS, resulting from short circuits current. The most significant source of dynamic power consumption is the switching activities of the charging and discharging load capacitances when the output changes between high and low logics [17, 18]. Since, there is a simultaneously finite rise and fall time for PMOS and NMOS, both of the transistors will be ON for a small period of time. Direct current flow from V_{DD} to ground creates a short circuit current. In one full cycle of CMOS logic, the current flows from the V_{DD} to load capacitance for charging and then applied to the ground during discharged. Therefore, in a complete cycle of charging and discharging, a

total of $Q = CL$. V_{DD} is removed from the V_{DD} to the ground. The performance of dynamic power consumption can be improved by evaluating Eq. (1).

$$P = \alpha CV^2 f \quad (1)$$

where, P is the power consumed, α the activity factor, C the switched capacitance, V the supply voltage and f the clock frequency. A clock in a system has activity factor of $\alpha = 1$, since it rises and falls every cycle. Mostly the activity factor of the data is 0.5. Dynamic power dissipation can be computed effectively if the right load capacitance estimated at the nodes and by factoring in the activity factors. It is crucial for designers and researchers to take static and dynamic power dissipations into consideration in designing low-power digital devices [19, 20]. Theoretically, dynamic logic has less power dissipated compared to static logic due to the absence of output glitch and capacitance reduction [21]. This can be deduced that dynamic CMOS logics are more beneficial than static CMOS logic. Nevertheless, the pre-charging operations that produce extra power dissipation do not influence the static CMOS logic. However the rapid changes in process technology cause the leakage power dissipation (static power) to increase much faster than dynamic power and found dominant over the time. Power dissipation per charge or discharge can be expressed by Eqs. (2) and (3).

$$P_{switch} = \frac{1}{2} C_{load} V_{DD}^2 \quad (2)$$

where, V_{DD} is the power supply voltage and

$$C_{load} = \sum_{i \in fanout} C_G^i + C_{wire} \quad (3)$$

given that C_G^i the gate capacitance of i_{th} fan-out and C_{wire} the capacitance of the driven connections [22]. Equations (2) and (3) show the relationship of total capacitance and supply power effecting the power dissipation. At the beginning, the power dissipation in CMOS devices is not a concern in chip design. The focus is more on system speed and reliability. However, in deep submicron technology, all consumed power commonly dissipated as heat and the cost of providing power has caused great interest in power reduction [23].

VLSI designers must keep the balance in power dissipation and the circuit's performance with scaling of the devices. Scaling methods play a significant role in reducing the power dissipation from one technology node to another node. There are various scaling methods used for VLSI circuits. Traditionally, most common are voltage scaling, load scaling, technology scaling and transistor sizing (width scaling). In voltage scaling for instance, supply voltage plays a vital role for controlling the power consumption and hence reducing the power dissipation. Moreover, threshold voltage of the device must be reduced proportionally as supply voltage reduces to sustain the transistor's output performance. The reduction in threshold voltage increases the leakage current drastically with each new technology generation.

The purpose of studying various scaling methods is to provide knowledge for scaling while keeping power dissipation and propagation delay in mind. There are techniques to minimise power dissipations and the possible control technique in CMOS logic as discussed in the following section.

3.1. Dynamic and static power simultaneous reduction by using mapping technique

Scan-based test is one of the chosen techniques to solve power problem. This method has become a popular design-for-test (DFT) procedure which gives low impact on the area and at the same time maintaining the circuit performance. A mapping technique was proposed by Sharif et al. [11] to block the scan chain transitions partially without affecting the circuit performance during normal operation as depicts in Fig. 2. Power dissipation suppressed the scan chain transitions near to the scan cell output by using multiplexers to block the scan chain transitions. It allowed desired values while scanning the vectors in the chain. Moreover, as the dominant portion of total power dissipation, static power dissipation can also reduce based on an input vector control technique combined with a method which reorders gate inputs. The pattern of input vector can be applied to the circuit through the set of controlled inputs during the scan mode. This work showed that it significantly reduced power dissipation during scan operations.

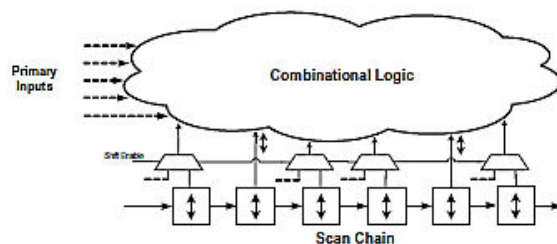


Fig. 2. Mapping technique [11].

Power dissipation improvement of the proposed technique was compared with the traditional scan structure for the verification purposes. C++ language was used and tested on ISCAS89 benchmarks where circuit technology library was mapped to a library. Table 1 shows the result of power dissipation of the proposed technique reported by Sharif et al. [11] compare to previous technique. The mapping technique successfully reduced both static and dynamic power dissipation without having any impact on test time. It also does not affect the maximum working frequency of the circuit, does not incur routing overhead and require no extra control signal since it uses the Shift Enable signal as its control signal.

Another technique using mapping approach method is also used by Dresig et al. for estimating and reducing the dynamic power dissipations of CMOS circuits [24]. Consider equation below

$$P_f = \sum P_i \quad (4)$$

where, $P_i = \alpha_i(k + fanout_i)$. Obviously, mapping strategy leads to reduced number of nodes in the circuit that result reducing P_f . The basic idea of this strategy is to include the P_i values as an optimisation criterion into the mapping process. This can be done by collapsing nodes with high P_i into internal nodes of complex gates. The method proposed by Dresig et al. [21] is efficient since they operate all logic level; no circuit level simulation is needed. They have found a value that

they called power factor P_f which takes into account to technology parameter k and suitable to compare different designs with regard to the average power dissipation. They have introduced a new mapping strategy, taking into consideration simulation results for minimising total power dissipation.

Table 1. Power dissipation of Sharif et al. and prior technique [11].

Traditional Scan Structure		Input Control		Proposed Structure (μW)		Improvement Compared with Traditional Scan (%)		Improvement Compared with Input Control (%)	
Dynamic (f) ($\mu\text{W}/\text{Hz}$)	Static (μW)	Dynamic (f) ($\mu\text{W}/\text{Hz}$)	Static (μW)	Dynamic (f) ($\mu\text{W}/\text{Hz}$)	Static (μW)	Dynamic	Static	Dynamic	Static
5.88E-8	27.99	5.72E-8	27.50	3.24E-8	23.89	44.82	14.65	43.23	13.12
6.43E-8	27.58	5.51E-8	26.69	2.38E-8	24.42	62.90	11.46	56.73	8.50
8.00E-8	33.72	6.92E-8	33.30	2.44E-8	27.99	69.44	17.00	64.67	15.95
8.46E-8	47.93	8.18E-8	47.50	8.22E-8	45.96	2.92	4.11	-0.41	3.24
5.69E-8	59.07	1.77E-8	56.97	1.78E-8	48.97	68.80	17.10	-0.50	14.05
6.30E-8	66.15	1.85E-8	64.90	1.82E-8	52.10	71.06	21.23	1.25	19.71
3.10E-8	115.54	3.06E-8	117.75	2.52E-8	95.78	18.61	17.09	17.50	18.65
3.19E-8	121.56	3.39E-8	124.75	2.59E-8	96.38	18.64	20.70	23.63	22.74
2.24E-7	128.22	1.93E-7	130.23	5.43E-8	117.00	75.77	9.02	71.83	10.43
3.56E-7	177.52	3.48E-7	179.86	3.52E-7	164.87	9.52	7.12	7.45	8.33
8.90E-7	327.52	1.29E-8	332.02	1.17E-8	315.00	98.68	3.82	9.50	5.12
1.50E-6	819.98	1.68E-8	854.52	1.57E-8	772.36	98.95	5.80	6.96	9.61

3.2. Optimisation technique

In 2008, Kabbani [18] developed a model and proposed an optimisation technique to minimise the power consumption. The model developed by normalising gate-switching power as a unit standard inverter and the effect of internal node capacitances counted accordingly. In this normalised switching power model, the first optimisation power technique was dealt with transistor sizing and creates a scheme according to a specific design goal. The second technique relies on the joint transistor sizing and supply voltage scaling for reducing the switching power dissipation under specific delay requirements. Concisely, power was widely known as

$$P = \alpha_g f_{clk} C_{out} V_{dd}^2 \tag{5}$$

where f_{clk} is the clock frequency and C_{out} is the output capacitance. Kabbani proposed expression is given by Eq. (6)

$$P_{nm} = \alpha_{nm} Z.(gh + p) \tag{6}$$

where α_{nm} is the normalised activity factor and is given as $\alpha_{nm} = \alpha_g/\alpha_v$, g is the gate logical effort with given $g = C_{ig}/C_{sv}$ and p is the parasitic power dissipation where p is given by $p = C_{ip}/C_{sv}$. The performance of the developed model in [18] has been tested in BSIM3v3 and UMC 0.13 μm technology by comparing modelling results with the simulation result produced by Specters and shown in Figs. 3 and 4.

Figure 3 shows that the dissipated power of a design is proportional to the total number of fanouts of the logic gates regardless the width of the buffer sizes. Fanout simply refer to the total number of gate inputs can feed from the output efficiently. In most designs, logic gates are connected to form more complex circuits. Since it is common for one output to be connected to several inputs, it is crucial for the logic gates to allow a certain number of gate inputs to be wired directly together without additional interfacing circuitry.

Fanout optimisation and sizing the buffers in a design is vital to satisfy the design constraints. This optimisation technique has successfully minimised the power consumption and saved power by about 20% more compared to the previous works [25]. Energy saving can achieved without delay penalty with equalisation of sensitivities to sizing, supply, and threshold voltage. Figure 4 shows this model produced a very good accuracy of the total power dissipation of various CMOS logic gates compare to the simulations.

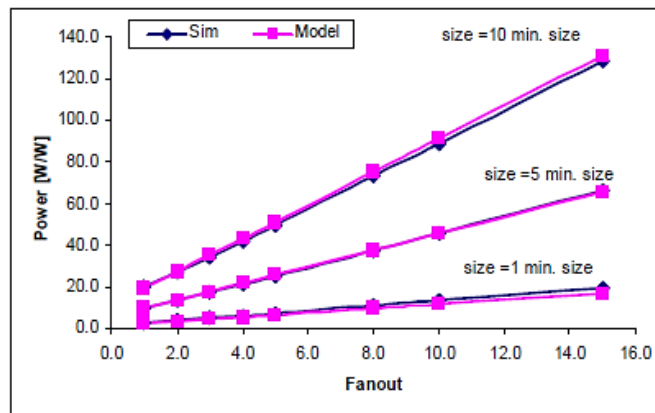


Fig. 3. A comparison between Kabbani proposed model and the BSIM3v3 for inverter with different sizes.

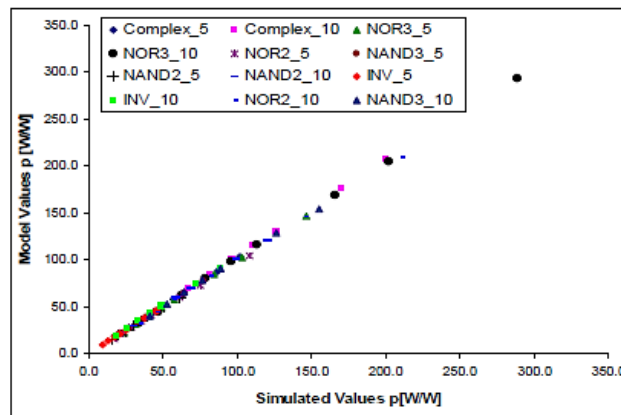


Fig. 4. The performance of the proposed model for different logic gates at different sizing and loading conditions.

3.3. Multi-threshold CMOS (MTCMOS) technique

MTCMOS utilised transistors with multiple threshold voltages (V_t) to optimise delay or power. Lower voltage devices were used on critical delay paths to minimise clock periods. Higher voltage devices were used on non-critical paths to reduce static leakage power without incurring a delay penalty. A common MTCMOS approach to reduce power is the utilisation of sleep transistors.

MOS current mode logic has been implemented in MTCMOS technology [26]. For decades, MTCMOS technology was used to reduce leakage in standby mode and reached high speed in active mode as shown in Fig. 5. In [26], the reduction of the operating supply voltage and level shifters eliminations were used as shown in Fig. 6. A high-speed 1:8 2.5 GbiVs demultiplexer was used as a test vehicle and 37% power saving was achieved. Furthermore, the MTCMOS design showed no impact over circuit parameters such as output impedance, gain, threshold voltage fluctuations and frequency response [26].

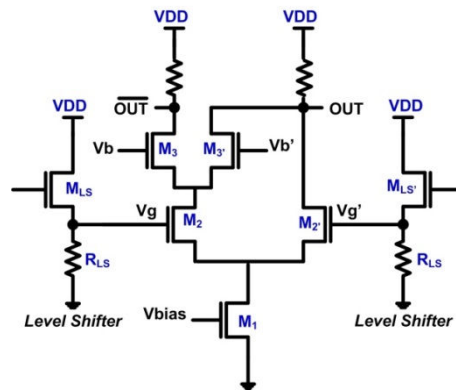


Fig. 5. MCML AND gate with level shifters (Conventional design).

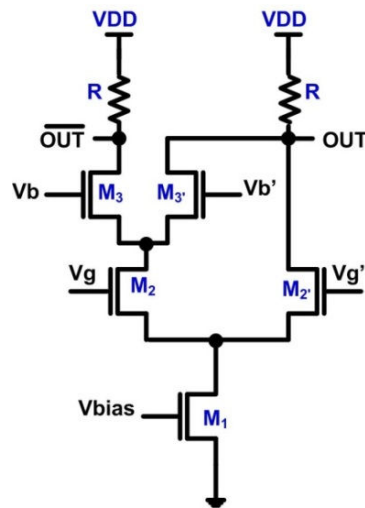


Fig. 6. MTCMOS MCML AND gate [26].

MTCMOS technique. The reason was that the current waveform data of a circuit were vectors while leakage current data of a circuit were scalars.

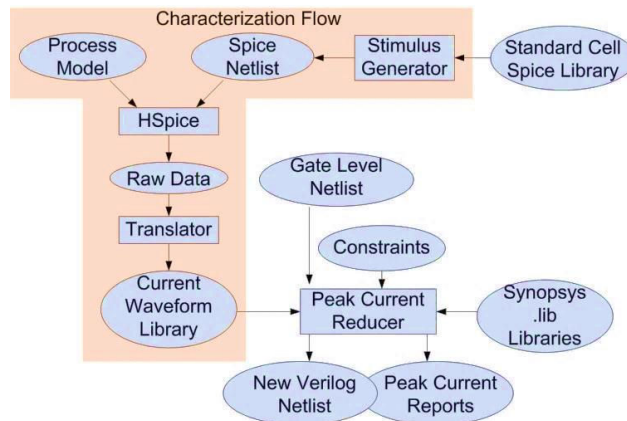


Fig. 8. Data flow for peak current reducer [27].

MTCMOS technique was also selected to reduce the leakage power of proposed 10 transistors full adder reported by Rani et al. [28]. A design with 10 transistors full adder used for low power operations has been implemented into different types of multiplier. All multipliers were developed in different process technologies including 90 nm, 70 nm, and 50 nm. MTCMOS logic was found effective standby leakage control technique, but difficult to implement since sleep transistor sizing was highly dependent on discharge pattern within the circuit block. Dual V_t domino logic could avoid the sizing difficulties and inherent performance associated with MTCMOS. High V_t cells were used to prevent leakage whereas low V_t cells were employed. Frequently, full adder used in the critical path to determine system overall performance. The comparison table of the work with the high transistor count and the existing 10-transistor adder is outlined in Table 2. The proposed adder is suitable for large multiplier circuits.

Table 2. Power savings with MTCMOS by Rani et al. [28].

Multiplier Type	Full Adder Type	Power (μ w) 90 nm	Power (μ w) 70 nm	Power (μ w) 50 nm
4×4 Conventional Array Multiplier	CMOS 28-T	67	292	63
4X4 Conventional Array Multiplier with MTCMOS	CMOS 10-T	24	77	10
Braun Conventional Multiplier	TG 18-T	64	295	63
Braun Conventional Multiplier with MTCMOS	CMOS 10-T	56	124	25
Baugh-Wooley Conventional Multiplier	TG 18-T	265	440	92
Baugh-Wooley Conventional Multiplier with MTCMOS	CMOS 10-T	162	132	23

3.4. Forward body bias technique (FBB)

Current through NMOS upsizing transistors decreases significantly and degrade the performance of circuits. On the other hands, more power is dissipated with the NMOS upsizing. Circuit design techniques should not only be focused on enhancing system speed but must also consider the power consumptions concurrently. A forward body bias technique for 65 nm CMOS technology can work under very low supply voltages (lower than $V_{DD} = 0.4$ V) has been proposed by Moradi et al. [29] as shown in Fig. 9. A domino logic circuit with constant supply voltage was used.

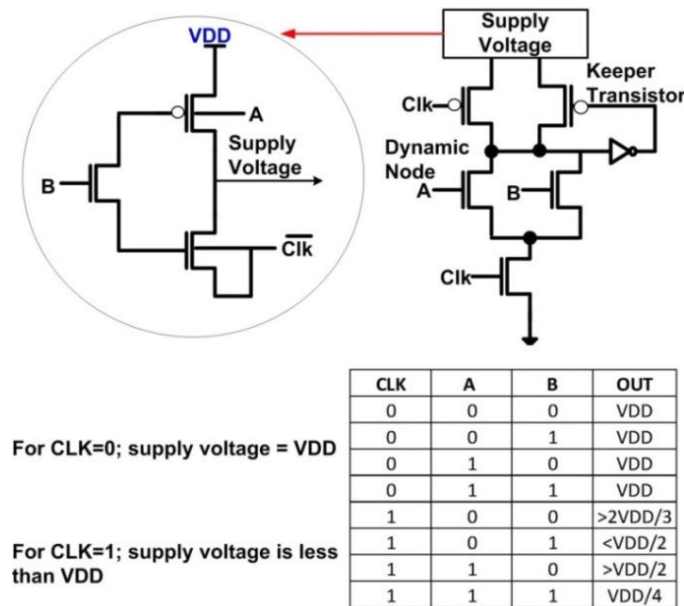


Fig. 9. Domino logic circuit by Moradi et al. [29].

For a clearer picture, Fig. 10 illustrates the operation of adaptive supply circuit. When "Clock" is low "0" whereby Clk_bar is in logic "1", the supply voltage node connects to the V_{DD} . When "inputs" are all logic low ("0"), the supply voltage decreases accordingly to reduce the power dissipation. Nevertheless, when supply voltage is low, the reliability and the sensitivity of the circuit input noise is deteriorates due to the reduction of on-current that passes through PMOS keeper transistor in order to hold the dynamic node state. In this work, NMOS device in the evaluation network are downsized to solve this noise issue.

A level shifter in TSMC 0.35 μ m process technology has been reported by [30] for comparison purposes by using the similar input parameter. Table 3 shows the proposed results of Moradi et al. with various bias voltages ranging from 0.1 V-0.5 V of power consumption and delay for modified level shifter designs. The proposed method reduced power consumptions significantly with a small delay smaller than the previous reported circuits. Power consumptions reduced significantly with the increase in reverse bias. Additionally, the slightly increase in delay caused the increase in reverse bias voltage.

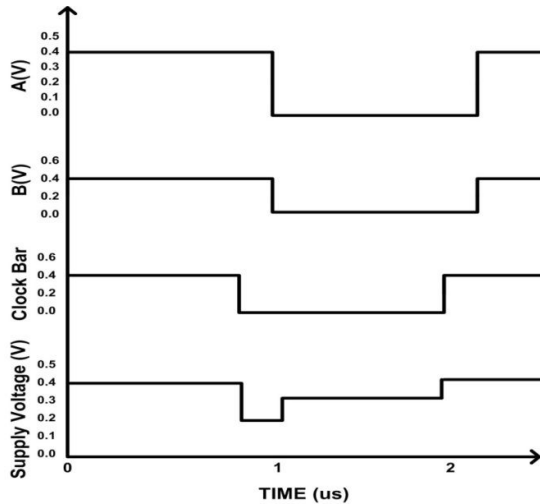


Fig. 10. Waveforms of adaptive supply voltage by Moradi et al. [29].

3.5. Hybrid network technique

A hybrid network technique in dynamic CMOS XOR / XNOR gate (DXG) based on 45 nm Berkeley short-channel IGFET Model (BSIM4 model) has been proposed by Wang et al. [31] to improve design signal skew. Moreover, it also improved the power consumption and drawn in small layout. The main objective was to investigate a better control of DXGP type which has greater leakage power compared to DXGN due to greater barrier height in PMOS compared to NMOS. On the other hands, DXGN has higher speed, thus the power consumption is high. Table 4 shows the normalised leakage current of the devices at 25°C, where the gate is static.

Table 3. Results of proposed level shifter circuit.

Bias voltage (V)	Level shifter configurations					
	Modified conventional type-I level shifter		Modified conventional type-II level shifter		Modified contention level shifter	
	Power Consumption (pW)	Delay (ns)	Power Consumption (pW)	Delay (ns)	Power Consumption (pW)	Delay (ns)
0.1	310.7590	2.7514	2209.7000	0.1120880	306.1605	0.3982240
0.2	205.6850	3.2149	1377.2000	0.1148531	201.0865	0.4048899
0.3	145.4804	3.6813	939.3620	0.1175174	140.8819	0.4117934
0.4	110.4990	4.4685	687.7304	0.1200811	105.9005	0.4198419
0.5	90.1250	5.3724	480.2857	0.1226488	85.5265	0.4275800

Table 4. Normalized leakage current of the devices at 25°C.

45 nm Technology	NMOS	PMOS
A: $I_{leak} (I_{sub}, I_{gate})$	37.12 (19.59, 17.53)	16.56 (15.56, 1)
B: I_{gate}	46.79	1.56

where Transistor: width = 1 μm , length = 45 nm, I_{leak} : Total leakage current current, I_{gate} : Gate leakage current, I_{sub} : Sub-threshold leakage current, $V_t = 0.22$ V, $V_{dd} = 0.8$ V, A: $V_{gs} = 0$ and $|V_{ds}| = V_{dd}$, B: $|V_{gs}| = |V_{gd}| = |V_{gb}| = V_{dd}$. Currents are normalised to the gate leakage current produced by PMOS Transistor in A state.

The hybrid network which has both PMOS and NMOS transistors in PDN applied instead of using the traditional PUN and PDN. Due to the input from with hybrid network (DXGH), both the static inverter and tilted input signal were cancelled. Hence, the power performance could be improved with an effective layout area. The structure of the proposed method is shown in Fig. 11.

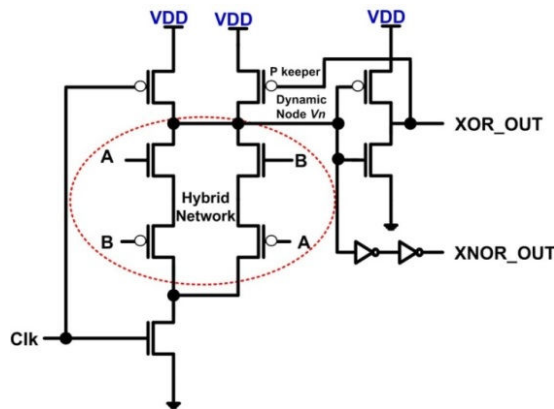


Fig. 11. The proposed method using DXGH by Wang et al. [31].

The removal of static inverter showed positive impact to the design such as less power consumption, non-skew input signals and smaller layout area. Figure 12 shows the comparison of the three different gates. The dynamic power, leakage power and layout area of DXGH and DXGN showed the reduction of 13%, 51% and 24% under similar delay time. The hybrid network utilisation has been traded off and eventually caused high power operation.

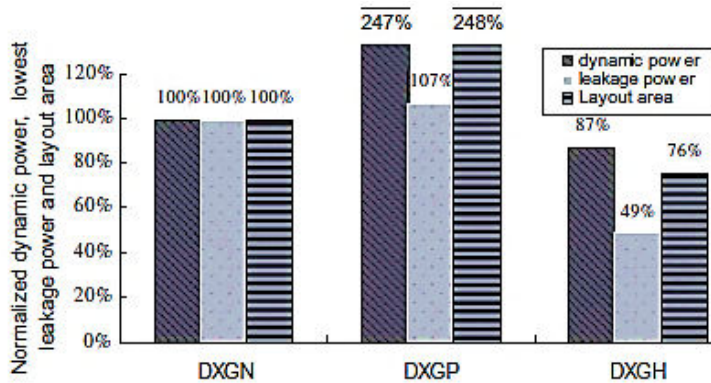


Fig. 12. Comparison of normalised active power, lowest leakage power and layout of different DXGs by Wang et al. [31].

The dynamic CMOS XOR/XNOR gate also showed superior robustness under process and temperature variation (PTV) which offered significant effect on leakage current. In order to evaluate the impact of PTV on leakage current and dynamic power characteristics of DXG, multiple-parameter Monte Carlo analysis is recommended.

3.6. Branch target buffer technique (BTB)

Three methods to reduce leakage power dissipated by using BTB is presented by Khan et al. [32]. The methods used are window, awake line buffer (ALB) and 2-level ALB (2L-ALB). The proposed methods are an important power components in modern processor where leakage power dissipation is part of total power dissipation. The findings showed that 2L-ALB reached additional reduction in leakage power with no performance loss compared to ALB method [32]. The extensive performance loss occurred due to the increment of propagation delay as V_{DD} approaches $2V_T$. The problem could be resolved by reducing the threshold voltage of the device. However, reducing the threshold voltage increases the subthreshold current, which is limited by acceptable leakage of static power dissipation [33]. 2L-ALB method can increase the power saving compared to other methods with no power penalty. Concisely, the work showed that the power dissipation in 2L-ALB reduced about 56% and the power dissipation of the entire BTB reduced by 35%.

Another method proposed by Sadeghi et al. [34] had successfully made two modifications on BTB to reduce the power consumed in the devices. Firstly, the size of the BTB was reduced by replacing the target address with relative distance between current instruction address and branch target address. BTB size reduction had reduced the static and dynamic power dissipations up to 3%. Secondly, a Next Branch Target (NBD) showed the distance between control flow instructions address and BTB. From the simulations, it showed that the method approached reduced power consumption up to 7.3%. Conversely, if combining these two techniques, the power dissipated about 8.3%. Figure 13 shows the new BTB structure for the first method of BTB size reduction and Fig. 14 shows a block diagram of NBD-based BTB architecture.

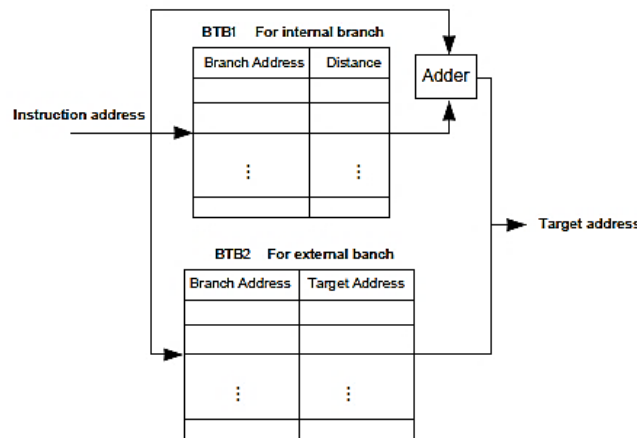


Fig. 13. Proposed BTB architecture composed of near and far BTB Part by Sadeghi et al. [34].

by Das et al. [36]. The proposed technique has successfully reduced the standby leakage and maintained the active-mode performance. MTCMOS technique has been used by Lu et al. reported in [27] where algorithms proposed to reduce the peak current. Their proposed technique with MTCMOS approach has successfully reduced the peak current up to 47% and also the leakage current. MTCMOS approach was also used Rani et al. [28] to reduce the leakage power by placing MTCMOS cell as a header and footer for the proposed 10 transistors full adder. The proposed technique has successfully improved the leakage power. However, Anis and Elmasry in [26] have a different approach from the reviewed works in implementing MTCMOS technique. MTCMOS was not used to reduce leakage power in the standby mode. Instead, it used to reduce the power supply and to ensure the correct function in active mode. The proposed work shown that 37% reduction in power saving and have no impact over circuit parameters.

FBB technique implementation in ultra-low supply voltages suitable for high speed circuits like domino logic circuit. The technique used to increase the speed while lower power dissipation is maintained by introducing lower supply voltages. The optimised bulk voltages discovered can boost the circuit to the maximum speed. The method proposed was found efficient as the little concession in delay has reduced the power significantly with the increment in reverse bias. Thus, NMOS upsized is not a mandatory to have successful evaluation.

In hybrid network technique, DXGH was used extensively especially in modern high performance microprocessor to decrease both leakage power and dynamic power about 51% and 13% respectively as compared to the DXGN. Thus, this approached success in achieving high power and speed operations without input signal skew.

The BTB technique reported that the leakage power dissipated in BTB reduced to 56% and BTB overall power reduction was recorded about 35%. The NBD-based BTB however consumed almost 7.3% of the processor power and the total energy gain has increased almost 8.3% in the microprocessor.

5. Conclusions

Various techniques used by researchers in order to get low power dissipations in CMOS technology. By reducing power dissipation, power consumptions can be optimised, thus make the electronic circuits more reliable. In this review, we presented a few techniques proposed by previous study such as mapping technique, optimisation technique, MTCMOS technique, forward body bias (FBB) technique, hybrid network technique and branch target buffer (BTB) technique and successfully reduced the power dissipation. This review serves its purpose to provide initial guideline for the researches.

References

1. Jalil, J.; Bin Ibni Reaz, M.; and Ali, M.A.M. (2013). CMOS differential ring oscillators: review of the performance of CMOS ROs in communication systems. *IEEE Microwave Magazine*, 14(5), 97-109.

2. Mohd-Yasin, F.; Khaw, M.K.; and Reaz, M.B.I. (2006). Radio frequency identification: Evolution of transponder circuit design. *Microwave Journal*, 49(6), 56-70.
3. Uddin, J.; Reaz, M.B.I.; Hasan, M.A.; Nordin, N.I.; Ibrahimy, M.I.; and Ali, M.A.M. (2010). UHF RFID antenna architectures and applications. *Scientific Research and Essays*, 5(10), 1033-1051.
4. Uddin, M.J.; Ibrahimy, M.I.; Reaz, M.B.I.; and Nordin, A.N. (2009). Design and application of radio frequency identification systems. *Journal of European Science Research*, 33(3), 438-453.
5. Teh, Y.K.; Mohd-Yasin, F.; Choong, F.; Reaz, M.I.; and Kordesch, A.V. (2009). Design and analysis of UHF micropower CMOS DTMOST rectifiers. *IEEE Transactions Circuits and Systems II: Express Briefs*, 56(2), 122-126.
6. Mohd-Yasin, F.; Yap, M.T.; and Reaz, M.B.I. (2007). CMOS instrumentation amplifier with offset cancellation circuitry for biomedical application. *WSEAS Transactions Circuits and Systems*, 6(1), 171-174.
7. Mohd-Yasin, F.; Khaw, M.K.; and Bin Ibne Reaz, M. (2006). Techniques of RFID systems: Architectures and applications. *Microwave Journal*, 49(7), 62-74.
8. Yasin, F.M.; Tye, K.F.; and Reaz, M.B.I. (2005). Design and implementation of interface circuitry for CMOS-based SAW gas sensors. *Proceedings of IEEE SOC Conference*, 161-164.
9. Khaw, M.K.; Mohd-Yasin, F.; and Reaz, M.B.I. (2004). Recent advances in the integrated circuit design of RFID transponder. *Proceedings of IEEE Semiconductor Electronics Conference*, 326-330.
10. Hanchate, N.; and Ranganathan, N. (2004). A new technique for leakage reduction in CMOS circuits using self-controlled stacked transistors. *Proceedings of VLSI Design Conference*, 228-233.
11. Sharifi, S.; Jaffari, J.; Hosseinabady, M.; Afzali-Kusha, A.; and Navabi, Z. (2005). Simultaneous reduction of dynamic and static power in scan structures. *Proceedings of Design, Automation and Test Conference*, Munich, 2, 846-851.
12. Ndubuisi, E.; and Etienne-Cummings, R. (2006). Power dissipation sources and possible control techniques in ultra-deep submicron CMOS technologies. *Microelectronics Journal*, 37(9), 851-860.
13. Elgharbawy, W.M.; and Bayoumi, M.A. (2005). Leakage sources and possible solutions in nanometer CMOS technologies. *IEEE Circuits Systems Magazine*, 5(4), 6-17.
14. Butzen, P.F.; Rosa Jr, L.S.; Chiappetta Filho, E.J.D.; Reis, A.I.; and Ribas, R.P. (2010). Standby power consumption estimation by interacting leakage current mechanisms in nanoscaled CMOS digital circuits. *Microelectronics Journal*, 41(4), 247-255.
15. Rabaey, M.; Chandrakasan, A.; and Nikolic, B. (2003). *Digital Integrated Circuits*. 2nd Edition, Pearson, New Delhi, India.
16. Roy, K.; Mukhopadhyay, S.; and Mahmoodi-Meimand, H. (2003). Leakage current mechanisms and leakage reduction techniques in deep-submicrometer CMOS circuits. *Proceedings of IEEE 91*, 2(2), 305-327.

17. Kabbani, A. (2008). Modelling and optimisation of switching power dissipation in static CMOS circuits. *IEEE Computer Society Annual Symposium*, 281-285.
18. Kabbani, A. (2010). Logical effort based dynamic power estimation and optimisation of static CMOS circuits. *Journal of VLSI*, 43(3), 279-288.
19. Chandrakasan, A.P.; Sheng, S.; and Brodersen, R.W. (1992). Low-power CMOS digital design. *IEEE Journal of Solid-State Circuits*, 27(4), 473-484.
20. Chandrakasan, A.P.; and Brodersen, R.W. (1995). Minimising power consumption in digital CMOS circuits. *Proceedings of IEEE*, 83(4), 498-523.
21. Macii, E.; and Poncino, M. (1996). Power consumption of static and dynamic CMOS circuits: a comparative study. *Proceedings in ASIC Conference*, 425-427.
22. Klab, S.; Napieralski, A.; and De Mey, G. (2009). Logi-thermal simulation of digital CMOS ICs with emphasis on dynamic power dissipation. *Proceedings of Mixed Design Integrated Circuits Systems*, 361- 365.
23. Romli, N.B.; Mamun, M.; Bhuiyan, M.A.S.; and Husain, H. (2012). Design of a low power dissipation and low input voltage range level shifter in Cedec 0.18- μm CMOS process. *Journal of World Applied Science*, 19(8), 1140-1148.
24. Dresig, F.; Lanches, P.; Rettig, O.; and Baitinger, U.G. (1993). Simulation and reduction of CMOS power dissipation at logic level. *Proceedings of Design Automation Conference*, 341-346.
25. Rezvani, P.; Ajami, A.H.; Pedram, M.; and Savoj, H. (1999). Leopard: a logical effort-based fanout optimiser for area and delay. *Proceedings of IEEE ICCAD Conference*, 516-519.
26. Anis, M.H.; and Elmasry, M.I. (2002). Power reduction via an MTCMOS implementation of MOS current mode logic. *Proceedings of IEEE ASIC/SOC Conference*, 193-197.
27. Lu, L.Y.; Wu, T.Y.; Chiou, L.Y.; and Shi, J.W. (2010). Peak current reduction using an MTCMOS technique. *Proceedings of Quality Electronic Design Symposium*, 255-259.
28. Rani, T.E.; and Rao, R. (2011). Area and power optimised multipliers with minimum leakage. *Proceeding of Electronics Computer and Technology Conference*, 3, 284-287.
29. Moradi, F.; Wisland, D.T.; Mahmoodi, H.; Cao, T.V.; and Dooghabadi, M.Z. (2009). Adaptive supply voltage circuit using body bias technique. *Proceedings of Mixed Design Integrated Circuits and Systems Conference*, 215-219.
30. Kumar, M.; Arya, S.K.; and Pandey, S. (2010). Level shifter for low power applications with body bias technique. *Journal of Engineering Science and Technology*, 2(6), 297-305.
31. Wang, J.; Gong, N.; Hou, L.; Peng, X.; Geng, S.; and Wu, W. (2011). Low power and high performance dynamic CMOS XOR/XNOR gate design. *Microelectronic Engineering*, 88(8), 2781-2784.
32. Kahn, R.; and Weiss, S. (2010). Reducing leakage power with BTB access prediction. *Journal of Integrated VLSI*, 43(1), 49-57.

33. Rabaey, J.M.; Chandrakasan, A.; and Nikolic, B. (2003). *Digital integrated circuits: A design perspective*. 2nd Edition, Prentice-Hall, Englewood Cliffs, NJ.
34. Sadeghi, H.; Sarbazi-Azad, H.; and Zarandi, H.R. (2009). Power-aware branch target prediction using a new BTB architecture. *Proceedings of VLSI-SoC Conference*, 53-58.
35. Changdao, D.; Graziano, M.; Sanchez, E.; Sonanza, R.M.; Zamboni, M.; and Zhifan, N. (2013). On the functional test of the BTB logic in pipelined and superscalar processors. *IEEE Test Workshop*, 1-6.
36. Das, K.K.; Lo, S.-H.; and Chuang, C.-T. (2006). High performance MTCMOS technique for leakage reduction in hybrid SOI-Epitaxial technology with enhanced-mobility PFET header. *Proceedings of IEEE 5th International on Embedded Systems and Design and 19th International Conference on VLSI Design*.